Chinese Chemical Letters 36 (2025) 110209

Contents lists available at ScienceDirect

Chinese Chemical Letters

journal homepage: www.elsevier.com/locate/cclet

Deep learning-based simultaneous bioavailability assessment and speciation analysis of dissolved organic copper

Zhaojing Huang[a,b,1], Hao Li[c,1], Jiayi Luo[b,d,1], Shunxing Li[b,e,*], Ming Zhao[b], Fengjiao Liu[b,e], Haijiao Xie[f]

[a] College of Chemistry and Chemical Engineering, Xiamen University, Xiamen 361005, China
[b] College of Chemistry, Chemical Engineering & Environmental Science, Minnan Normal University, Zhangzhou 363000, China
[c] College of Computer and Data Science/College of Software, Fuzhou University, Fuzhou 350108, China
[d] School of Energy and Environmental Engineering, University of Science and Technology Beijing, Beijing 100083, China
[e] Fujian Province Key Laboratory of Modern Analytical Science and Separation Technology, Fujian Province University Key Laboratory of Pollution Monitoring and Control, Minnan Normal University, Zhangzhou 363003, China
[f] Hangzhou Yanqu Information Technology Company of Limited Liability, Hangzhou 310003, China

ARTICLE INFO

Article history:
Received 6 May 2024
Revised 25 June 2024
Accepted 2 July 2024
Available online 4 July 2024

Keywords:
Metal bioavailability
Metal speciation
Primary productivity
Intelligent analysis
Biomimetic sensor

ABSTRACT

Algal copper uptake (*i.e.*, Cu bioavailability) in the euphotic zone plays a vital role in algal photosynthesis and respiration, affecting the primary productivity and the source and sink of atmospheric carbon. Algal Cu uptake is controlled by natural dissolved organic Cu (DOCu) speciation (*i.e.*, complexed with the dissolved organic matter) that conventionally could be tested by model prediction or molecular-level characterizations in the lab, while DOCu uptake are hardly directly assessed. Thus, the new chemistry-biology insight into the mechanisms of the Cu uptake process in algae is urgent. The DOCu speciation transformation (organic DOCu to free Cu(II) ions), enzymatic reduction-induced valence change (reduction of free Cu(II) to Cu(I) ions), and algal Cu uptake at the algae-water interface are imitated. Herein, an intelligent system with DOCu colorimetric sensor is developed for real-time monitoring of newly generated Cu(I) ions. Deep learning with whole sample image-based characterization and powerful feature extraction capabilities facilitates colorimetric measurement. In this context, the Cu bioavailability with 7 kinds of organic ligands (*e.g.*, amino acids, organic acids, carbohydrates) can be predicted by the mimetic intelligent biosensor within 15.0 min, *i.e.*, the DOCu uptake and speciation is successfully predicted and streamlined by the biomimetic approach.

As an essential micronutrient, Cu is essential for ensuring proper functioning of algal photosynthesis and respiration [1], and then the primary productivity. Algal Cu uptake in the euphotic zone is important [2], because the euphotic zone with lots of oxygen, free radicals, and dissolved organic matter (DOM) is the most bio-active region for the metal biogeochemical cycle [3]. Hence, algal Cu uptake can affect the source and sink of atmospheric carbon in the euphotic zone. Algal bioavailable Cu uptake requires that Cu(II) is reduced to Cu(I) (chemical valence change) prior to transport across the algal cytomembrane [4,5]. In this case, the extracellular reduction, *i.e.*, Cu(II) reduced to Cu(I), is critically essential, because most of the DOCu exists in the oxidation state Cu(II) with organic ligands in the euphotic zone (oxygen-enriched waters), with only minor amounts of Cu(I) or inorganic state [5,6]. In the euphotic zone, DOCu complexes are degraded by reactive oxygen species (ROS) (*e.g.*, from O_2, H_2O, or cell-released), generate Cu(II), and reduced to Cu(I) by reduced coenzyme (NADPH/$NADP^+$) [7]. Cu-internalization is mainly thought to occur *via* Cu(I)-specific transporters (ToCTRs), which are transcriptionally regulated by Cu availability, as shown in Fig. S1a (Supporting information) [5]. The photodegradation of organic ligands from DOCu and enzymatic reduction of Cu(II) are the pivotal factors in DOCu uptake and carbon fixation for eukaryotic phytoplankton and the primary productivity.

The bioavailable DOCu speciation is dominated by organic complexes at algae-water interface [8]. The foremost factor influencing metal speciation and metal transport from freshwater systems to the sea is functional groups of humic substances and DOM [9-12]. Currently, the DOCu complexes characterization can be gained generally *via* molecular-level characterizations, *e.g.*, UV/Vis, liquid chromatography-mass spectrometry, ion mobility spectrometry-

* Corresponding author.
E-mail address: lishunxing@mnnu.edu.cn (S. Li).
[1] These authors contributed equally to this work.

https://doi.org/10.1016/j.cclet.2024.110209
1001-8417/

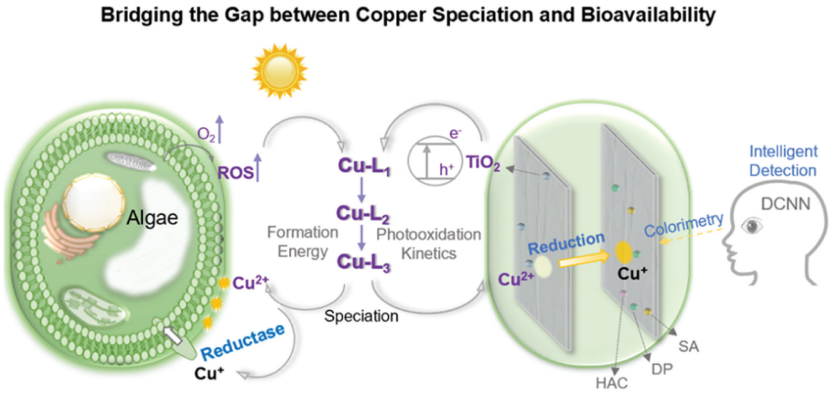

Fig. 1. Simulation of DOCu organic ligands photodegradation, valence change, and uptake at algae-water interface.

mass spectrometry, but analyzing the multi-molecular complexes remains a challenging task, particularly to identify and measure dominant weak ligands in the ocean [13,14]. With the increasing emphasis on metal speciation and toxicity, copper speciation was being incorporated into water quality criteria and the aquatic environment quality standard, based on model prediction (*e.g.*, the biotic ligand model, nonideal competitive adsorption, Stockholm humic model, or WHAM-Windermere humic aqueous model) in specific waters [15-19]. According to the designed spectral empirical parameters, the special sample preparation procedures are used by the above models in the lab, which could cause significant differences in the field studies [20]. The above studies highlight a great demand for metal speciation easy-to-use measurement in waters. As such, the presence of natural organic ligands is important in assessing the bioavailable DOCu [21]. For organic Cu bioavailability, the extracellular degradation (*i.e.*, DOCu species transformation from organic Cu-Ligands (Cu-$L_{1\sim X}$) into inorganic Cu(II) ions), the reduction of Cu(II) to Cu(I) (*i.e.*, enzymatic reduction-induced valence change) all played a key role in DOCu uptake on the algae-water interface. However, such information could be obtained from the proposed approach based on the chemistry-biology mechanisms of the Cu uptake process.

Thus, DOCu chemical speciation assessment must respond to the demand for DOCu bioavailability assessment. There is a consensus that biological problems can be solved by imitating biological structures within the bioreactor and biosensors [22]. For instant monitoring of the nascent bioavailable Cu(I) in the euphotic zone, on-site biosensors of algal DOCu bioavailability-based speciation assessment are proposed. The biochemical process of DOCu in Fig. 1 is imitated with the photodegradation of organic ligand in acidic condition assisted by salicylic acid (SA), reduction of photogenerated Cu(II) into Cu(I) with hydroxylamine hydrochloride (HAC), and colorimetric reaction between 2,9-dimethyl-1,10-phiroline (DP) and Cu(I), respectively. However, the noise influence of environmental factors on color development calls for new in visual detection methods. As a newly developing nonparametric approach, deep learning (DL) methods are efficient in dealing with heterogeneous data and in finding relationships between countless information [23,24], to assess the characteristics and health impacts of air pollution [24] and predict adverse effects of metallic nanomaterials to various aquatic organisms [25]. In photodegradation- colorimetric detection, it is necessary for real-time monitoring of newly generated Cu(I) accurately. Hence, the deep convolutional neural network model (DCNN) is selected and combined with the time-lapse camera without manual input to effectively predict Cu(I) concentration per minute *via* colorimetric measurement, for its excellent performance in powerful feature extraction capabilities, dynamic image recognition, and high-throughput data processing [26-28]. This new approach enables autonomous identification of nascent Cu(I) (*i.e.*, bioavailable Cu) from specific DOCu speciation, based on the photodegradation kinetics [28]. Accordingly, with the help of analytical tools, high-dimensional features, and real-time speciation can be identified, thus giving solid support to the DOCu bioavailability assessment.

Due to the extracellular matrix having a filamentous architecture, Cu and DOCu complexes can enter the cytomembrane through DOCu degradation, Cu(II)-Cu(I) reduction, and transmembrane transport by ToCTRs [5]. Herein, a nano filamentous sensor with photocatalyst (Titanium dioxide, TiO_2) [29], enzymatic reductants (HAC) [30,31], and hydrophilic surfactant (polyvinylpyrrolidone, PVP) is programmed to mimic membranal Cu-uptake process. Meanwhile, as a colorimetric probe, DP is selected for its strong affinity with Cu(I) [32]. In this study, Cu(II) can be reduced to Cu(I) by HAC and chelated by DP for color development. A mimetic intelligent biosensor is proposed for DOCu speciation, bioavailability, and carbon fixation efficiency assessment, as shown in Fig. 1.

The euphotic zone in the inshore areas and estuaries is usually characterized by high concentrations of DOM from both allochthonous and autochthonous sources [33], including biological productivity and anthropogenic input (*i.e.*, the primary products, secondary metabolites, and synthetic chelators), which could bind 99% of dissolved Copper [34]. According to the reported results [35,36], 5 types, and 7 ligands are selected as the representatives of dissolved organic ligands at algae-water interface in euphotic zone, including organic acids (oxalic acid, citric acid), carbohydrates (D-glucuronic acid), urea, EDTA, amino acids (L-glycine, L-methionine), as shown on Fig. S1b (Supporting information). Organic acids, carbohydrates, and amino acids are some of the main components of DOM and humic substances from biological production or metabolism, which are widely distributed in water. Urea is the final metabolite of organic nitrogenous compounds and also one of the components of DOM. EDTA, a strong metal chelator, is representative of artificial synthesis and industrial wastewater flowing into natural seawater [36].

A stable polymer material (polyacrylonitrile, PAN) is selected as the load base of the functional material with hydrophilic surfactant PVP. Electrospinning technique is chosen to manufacture the biosensors with both pretreatment and colorimetric detection capabilities due to its superior nanofiber-weaving capabilities. The biomimetic sensor, *i.e.*, PAN-DSH@TiO_2 is prepared as follows. Add PAN (0.30 g), PVP (0.10 g), DP (0.20 g, chromogenic agent), hydroxylamine hydrochloride (0.03 g, reductant), salicylic acid (0.05 g, acid reagent), and dimethyl formamide (DMF) (5.0 mL) are added into bottle A and then the mixture is heated at 50.0 °C until evenly mixed. After adding PAN and PVP into bottle B, TiO_2 (0.07 g, photocatalyst) is added and this mixture is also heated in DMF solvent at 50.0 °C. After stirring respectively and evenly, the solutions from

bottles A and B are successively loaded into the injector and electrospun at the pushing speed of 1.0 mL/h and voltage of 16.0 kV for the preparation of the bilayer sensor. The TiO_2 and DP are distributed in different layers to avoid the photodegradation of DP.

Solar-irradiated photodegradation of DOCu organic ligands in the euphotic zone is imitated, using a xenon lamp (ozone-free) with fixed light intensity (4500 Lux), electric power (50 W), current (14 A), and illumination working wavelength (420–770 nm) at a fixed distance (10 cm) upon the test paper. For the construction of Cu(II) intelligent colorimetric system, each Cu(II) solution (1.00–200.00 μmol/L, 30.0 μL) is dropped onto the PAN-DSH@TiO_2 test paper (1.0 cm^2), 30 parallel pictures are captured by a time-lapse camera, without manual input to capture three pictures per minute that effectively determine Cu(I) concentration *via* colorimetric reaction, the environmental parameters, such as illumination intensity, can be fixed on the machine vision system (R = 20, G = 20, B = 20). Six thousand sample pictures are uploaded for training the DCNN model.

Marine phytoplankton *Conticribra Weissflogii* (CCMA-102) is cultured using a modified f/2 media in artificial seawater, pH 8.1, at a salinity of 35. All the vessels are soaked in 5% HNO_3 for at least 12 h and washed with ultrapure water 3 times before use. The Cu(II) ions (7.28 μg/L) are combined with different organic ligands (L-methionine, urea, oxalic acid, citric acid, EDTA, D-glucuronic acid, or L-glycine, 100.0 μmol/L) for 4 days as algal culture medium. Algae with 6.25 × 10^4 cell/mL density are placed in an incubator with constant light (92.59 μmol m^{-2} s^{-1}) and fixed temperature (25.0 °C), grown on a 12:12 h photoperiod. For the calculation of algae growth rate, cell density is obtained using a fluorescence spectrophotometer (Agilent). Algal growth rate constant is estimated using linear regression of natural-logarithm-transformed cell density *versus* growth time, which the above computational formula is shown in Eqs. S1 and S2 (Supporting information). For calculation of Cu-uptake rate, each algal culture media (5.0 mL) is filtered with 0.22 μm membrane, added into Teflon cans with 65% nitric acid and 30% hydrogen peroxide solutions, and digested with microwave digestion system for 30 min. The concentration of Cu in algal culture media, *i.e.*, unabsorbed Cu, is determined with ICP-MS (Agilent), the total algal Cu uptake could be calculated *via* concentration gap and corresponding sample volume. On this basis, algal Cu uptake per cell could be further calculated through cell density and corresponding sample volume.

Except as an efficient and environmentally-friendly sample pretreatment technology, the photodegradation is selected for mimetic species transformation of DOCu on the algae-water interface in the euphotic zone. In the acidic medium, *i.e.*, the coexistence of salicylic acid, the heterogeneous interface of TiO_2 nano-particles has abundant electron holes (h^+) and positive electricity (isoelectric points = 6.2) for attracting organic ligands, DP only specifically binds to Cu(I) as a specific chromogenic probe, *i.e.*, newly generated Cu(I) could be determined when Cu(II) is reduced into Cu(I) and HAC (*i.e.*, auxiliary reagents) to imitate the enzymatic reduction-induced valence change. The chromogenic agents and auxiliary reagents (or the photocatalysts) are fixed respectively into the fibrous, hydrophilic, and stable polymer substrate (*i.e.*, PAN/PVP film) by bilevel assembly and electrospinning (as shown in Fig. 1). *Via* PAN/PVP encapsulation, nano TiO_2 agglomeration and auxiliary reagents oxidation could be prevented, as shown in Figs. 2a and b. The sensor is labeled as PAN-DSH@TiO_2, with a similar specific surface area (10.0804 m^2/g) as the cytomembrane (shown in Fig. S2 in Supporting information).

As seen in Fig. 2a, the polymer fiber of PAN-DSH is smooth, which indicates that salicylic acid, hydroxylamine hydrochloride, and DP could be effectively dispersed into PAN/PVP during the preparation and spinning process. When TiO_2 is mixed with PAN/PVP and uploaded onto the PAN-DSH as the upper layer of

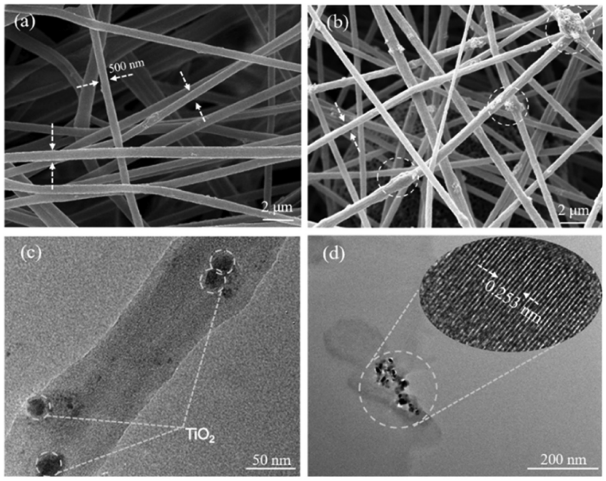

Fig. 2. SEM of PAN-DSH (a) and PAN-DSH@TiO2 (b, c) and TEM of PAN-DSH@TiO2 (d).

PAN-DSH@TiO_2, its protrusion, particle size (25 nm), and crystal face (101) can be observed in Figs. 2b-d. Because the pack of TiO_2 with PAN is firm, TiO_2 nanoparticles cannot be separated from the PAN/PVP substrates even after ultrasonic dispersion for 10.0 min. Therefore, the reproducibility in the manufacturing process of our sensor (PAN-DSH@TiO_2) could be ensured. The sample solution with organic DOCu could penetrate sequentially into the photocatalytic layer and then the chromogenic layer for the guiding and dissolving of PVP as a hydrophilic surfactant. After the dissolving of PVP, TiO_2 as the photocatalyst could be bared, DP and the auxiliary reagents could be released, and then their functions could be effective.

In this sensor, detectable Cu(I) almost comes from the reduction of Cu(II) by HAC, due to 99% of DOCu in natural water being Cu(II), and then chelated with DP for Cu(II) detection. Accordingly, the anti-interference ability of our sensor for selective determination of Cu(II) is excellent, under the paper-based reaction conditions. After reaction with Cu(II) (1.0 mg/L), the influence of coexisting ions (19 kinds, shown in Fig. 3a) on the color and gray value change (ΔG) on PAN-DSH@TiO_2 is not obvious (seen in Fig. 3a), *i.e.*, Cu(II) could be selectivity determined by our colorimetric detection-based sensor.

In exploring the degradation kinetics of DOCu speciation in natural water under light, the colorimetric development method and DCNN model are adopted to measure the nascent reduced Cu(II) ion concentration. With whole sample image-based characterization and powerful feature extraction capabilities [37], this model could randomly extract known samples, learn and discriminate by convolution and pooling, and obtain features extraction and cyclic learning map of 6000 samples. Combining the DCNN model, the colorimetric detection has competitive advantages, including quick detection (≤2 s), more accurate (~100%, after 300 training epochs), and wide detection range (1.0–200.0 μmol/L), however the detection time and limit of traditional UV–vis spectroscopy are 5 min and 0.47 μmol/L (Water quality—Determination of copper—2,9-dimethy-1,10-phenanthroline spetrophotometric method, HJ 486–2009) and 0.94 μmol/L (Water quality–Determination of copper—2,9-dimethy-1,10-phenanthroline spectrophotometric method, GB/T 7473–1987), respectively, as shown in Fig. 3b. Herein, combining the hydrophilic and stable chemosensor (effectiveness insurance), industrial camera (photo-capture stability), and DCNN model (powerful feature extraction), the concentration of Cu(II) ions degraded from Cu-L_x (seen in Fig. 3c) can be effectively predicted *via* intelligent colorimetric detection (as shown in Figs. 4a and b), thus replacing the traditional visual detection.

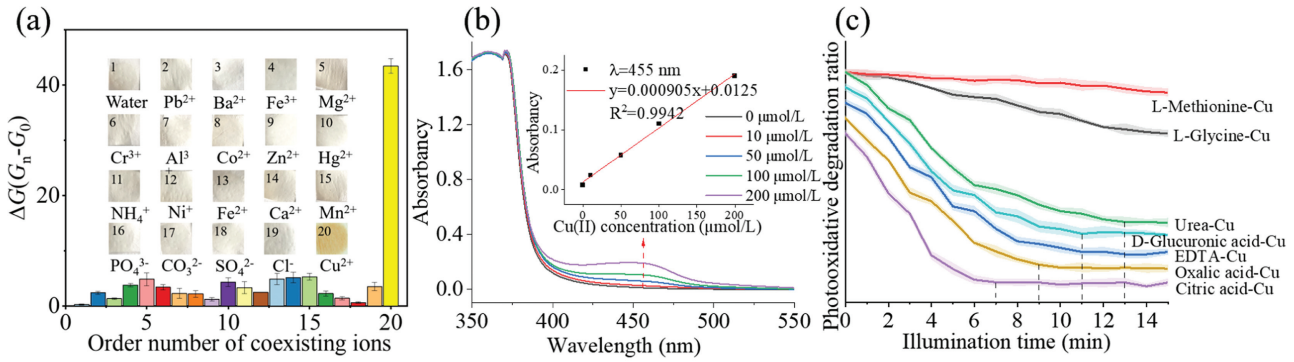

Fig. 3. Color and gray value change (ΔG) on PAN-DSH@TiO_2 after reaction with Cu(II) (1.0 mg/L) under the coexisting of 19 kinds ions (1.0 mg/L) ($n = 3$) (a), traditional visual detection of Cu(II) by 2,9-dimethyl-1,10-phiroline with UV–vis spectrum (b), and photodegradation ratio *vs.* illumination time for different DOCu on PAN-DSH@TiO_2 (c).

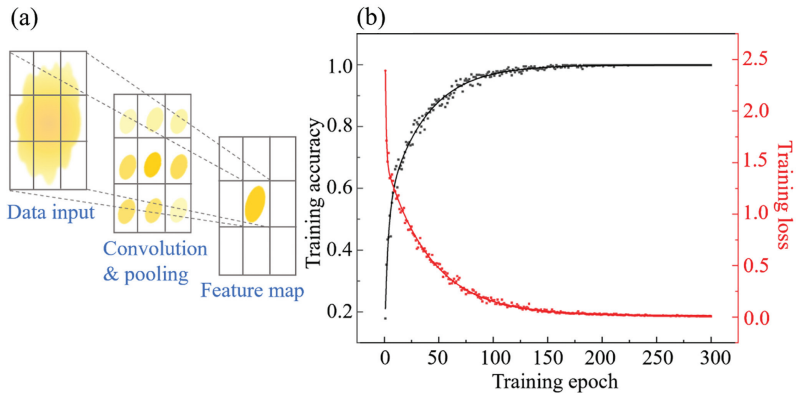

Fig. 4. Visual signal learning by DCNN (a), variation curve of training accuracy and loss with the increase of training epoch (b).

Seven natural organic ligands are selected as the representative components of humic substances and DOM. Most copper tends to bind with thiols, such as amino acids (-SH), peptides, and proteins in waters and organisms, so L-methionine is selected as the representative of such substances [29]. As a representative of common amino acids, L-glycine is mainly compared with amino acids with -SH groups. Urea is the final product of protein with $-NH_2$ degradation and widely exists in nature, selected as the representative of small molecules of nitrogenous organic matter. Copper is more likely to combine with monosaccharide acids, so D-glucuronic acid is selected. Oxalic acid is a carboxylic acid that widely exists in water and plants, and it is also representative of organic acid with the minimum molecular weight. Citric acid with many carboxyl groups (3 carboxyl + 1 hydroxyl group), is also commonly found in nature. The comparison between citric acid and oxalic acid (2 carboxyl group) can explore the binding stability of carboxyl groups to Cu(II) ions.

To promote the electrostatic attraction between organic ligands and Cu(II) ions (1.0 mmol/L), the ligand solutions (10.0 mmol/L, seen in Fig. 3c), including amino acid (L-methionine and L-glycine), organic acid (oxalic acid and citric acid), synthetic chelate (EDTA), carbohydrate (D-glucuronic acid), and nitrogen metabolites (urea) are prepared respectively at pH 4-6 for their isoelectric points < 6, *i.e.*, the organic ligands are existing as anions. The Cu(II) ions are bound with organic ligands at 20:1 in the seawater (10.0 mL, TOC = 10.7 mg/L, pH 8.1) under 25.0 °C for 6 h and then their complexation equilibrates could be obtained through instant monitoring of the free Cu(II) ions with our sensor. Then, the degradation kinetics of the copper complex can be calculated by the color difference by 'before' and 'after' photodegradation under sunlight exposure (92.59 μmol m^{-2} s^{-1}, λ = 420–770 nm).

The copper complex solutions (30.0 μL) are added onto PAN-DSH@TiO_2 paper and their fast color signals (<2 s) are recorded to calculate the photodegradation kinetics, *i.e.*, the photodegradation rate of organic ligands from DOCu, as shown in Fig. 3c and Table 1. Under the irradiation of a fixed light source, the color of PAN-DSH@TiO_2 paper gradually changes with the increasing illumination time for the photodegradation of DOCu and the color is basically stable and unchanged after 15.0 min, except for L-methionine. The photodegradation kinetics is different for different DOCu speciation. The degradation of Cu citrate, oxalate, D-glucuronic acid, EDTA, urea, L-glycine, and L-methionine could be basically completed within 7.0, 9.0, 11.0, 11.0, 13.0, 15.0, and 40.0 min, respectively, with different degradation ratio (98%, 95%, 95%, 95%, 94%, 47%, and 30%) and kinetic constant (0.537, 0.367, 0.281, 0.328, 0.283, 0.037, and 0.00879) as shown in Fig. 3c, Fig. S3 (Supporting information) and Table 1.

The dissolved Cu organic acids, urea, and monosaccharides are easy to be photodegraded and then free Cu(II) ions are released [7]. According to the theory of hard and soft acids and bases (HSAB), the strength differences of the bond between Cu(II) and different ligands are due to the molecular structure, coordination sites, and electron donating ability [28]. The molecular structure of the ligand is shown in Fig. S1b (Supporting information). Both the ordinary amino acids (L-glycine) and the sulfur-containing amino acid (L-methionine) are difficult to be completely photodegraded in a short time (>15.0 min) because L-glycine and L-methionine have two (-COOH and $-NH_2$) and three (-COOH, $-NH_2$, -SH) binding sites, with copper for forming a stable circular structure. Carboxylic acids (citric acid and oxalic acid) have more electronegative carboxylic groups, but their electron donation trend is relatively weak, and hardly provides coordination electrons to Cu(II) ions that are easier

Table 1
Photodegradation kinetics constant (PKC), Cu-uptake rate constant (CuRC), Growth rate constant of algae (GCA), and configurational formation energy (CFE) of DOCu organic ligands.

Types	Organic ligands	Algal Cu uptake			Photodegradation kinetics
		CFE (kcal/mol)	GCA (10^3 cell mL^{-1} h^{-1})	CuRC (10^{-7} pg $cell^{-1}$ h^{-1})	PKC (μmol/min)
Amino acid	L-methionine	-273.38	2.8583	3.7128	0.00879
	L-glycine	-229.68	2.9469	4.0876	0.0370
Amino-polycarboxylate	EDTA	-158.24	4.1344	6.3699	0.328
Nitrogen metabolites	Urea	-213.37	3.3979	4.9465	0.283
Carbohydrate	D-glucuronic acid	-229.89	3.6656	5.9938	0.281
Organic acid	Oxalic acid	-185.33	3.8312	6.3817	0.367
	Citric acid	120.37	4.1302	6.6797	0.537

to be photodegraded in water. Citric acid has stronger electronegativity and electron stealing tendency than that of oxalic acid for the difference of their carboxyl groups (3:2). Due to EDTA having 4 carboxyl groups bonds to 2 nitrogen atoms, the electron cloud density of carboxyl group increases and the electron donating ability is stronger [39] There are carboxyl groups binding to 4 electron-donating groups of hydroxyl groups in D-glucuronic acid, the binding sites of Cu(II) ions and D-glucuronic acid are presumed to be mono-carboxyl groups by electrostatic attraction, and the electronegativity is weaker than that of organic acids, and the binding ability with Cu(II) is slightly stronger. Urea is the smallest nitrogen-containing molecule, can be bound with copper due to the amino groups and carbonyl groups, and has a strong deformability and electron-donating ability to bind with Cu(II) ions. Amino acids are generally bound with Cu(II) ions by amino and carboxyl groups. Compared with hydroxyl groups of citric acids, urea, and EDTA, the hydroxyl groups of amino acids have stronger electron donating ability and cloud density, so the complex stability of amino acids-Cu(II) is strong. The sulfur atom in the sulfur-containing amino acids can provide Cu(II) ion binding electronic [6], *i.e.*, the combination of L-methionine and Cu(II) ions has the possibility of tridentate chelate with a stronger bond. Accordingly, L-methionine is more difficult to degrade than common acids, and the degradation rate is estimated to be 30% within 40 min. Hence, the stability of binding with copper ions based on HSAB theory, is listed in this order: citric acid < oxalic acid < EDTA < D-glucuronic acid < urea < L-glycine < L-methionine.

According to the electron-donating capacity and HSAB theory, copper complexes have different stability due to different structures, which can be reflected by their PKC. According to density functional theory (DFT), the CFE for 7 Cu ligands are calculated by the Gaussian09 program package, whose details are shown in Eq. S4 (see Formulae and Equations in Supporting infoamation). The correlation coefficient between DOCu PKC and CFE is 0.793. Thus, HSAB and DFT theory confirm the relationship between photodegradation kinetics and DOCu photostability, the copper uptake process strictly affects the carbon fixation effect of primary productivity.

Due to DOCu can enter the cytomembrane through DOCu degradation (*i.e.*, organic-Cu into inorganic-Cu), enzymatic reduction of Cu(II)-Cu(I), and transmembrane transport *via* Cu(I)-specific transporters. The scientific aspects of speciation analysis of dissolved organic ligands and copper ions in this study facilitate the environmental problems solving of the metal uptake within algal photosynthesis and carbon migration, which supports the assessment of the metal bioavailability of algae at the presence of DOCu. Both theory and practice have been proved, this approach proposes an innovative biomimetic workflow for the chemistry-biology insight of the metal uptake process and could be easily extended to other metal uptake.

As a frequently-used marine diatom model [38], Conticribra weissflogii (CCMA-102) is proposed for the bioavailability assessment of different DOCu speciation. Cu-internalization is mainly thought to occur *via* ToCTRs. In the algae-water interface, DOCu organic ligands are photodegraded by ROS, and then the generated Cu(II) ions are reduced to Cu(I) by NADPH/$NADP^+$. The DOCu-uptake rate (CuRC, shown in Fig. 5a and Table 1) can be predicted for 4 days with a correlation coefficient (CRE) of 0.929. These results prove that the DOCu bioavailability is controlled by DOCu speciation, which could be predicted by the mimetic function of cytomembrane, *i.e.*, biosensor based on DOCu photodegradation and Cu(II) reduction. Because the ROS yields from TiO_2 are more than that from the euphotic zone *via* photocatalysis, the experimental time could be reduced for Cu speciation and bioavailability assessment from 4 days to 15.0 min, and carbon fixation efficiency in Cu-induced primary productivity can be assessed quickly.

Meanwhile, the CuRC is highly correlated with the photodegradation kinetics of organic Cu (CRE 0.929) (Fig. 5b and Table 1), because algal photosynthesis and respiration are affected by DOCu bioavailability. The photostable ligands (L-glycine and L-methionine) reduce DOCu bioavailability and thus algal growth rate, organic ligands degraded easily (*e.g.*, citric acid or oxalic acid) have little effect on algal Cu uptake (Fig. 5c and Table 1). Thus, the biomimetic sensor designed with high Cu-uptake-process-related specificity can yield reliable Cu-bioavailability results, which can be used as the bridge between DOCu speciation and bioavailability for the first time.

DOCu uptake of algae can affect primary productivity and even the source and sink of atmospheric carbon in euphotic zone. For organic DOCu bioavailability in the euphotic zone, both the extracellular photodegradation and the enzymatic reduction-induced valence changes play a pivotal role in DOCu uptake at the algae-water interface. For exploring the mechanism of copper absorption, the photodegradation kinetics of dissolved Cu were explored by the biomimetic sensor that simulates the photodegradation process and enzymatic reduction at the algae-water interface. Since the dissolved copper is tightly bound to DOM in oxygen-rich waters, Cu uptake by primary productivity is mainly *via* Cu(I)-specific transporters, we systematically studied the mechanism of Cu entering into algal cells, and found that the order of Cu entering into algal cells bound to organic ligands was closely related to the photodegradation rate of Cu organic complexes, and the Cu-transition of organic and chemical valence states was the key to the algal Cu uptake.

For instant monitoring of the biochemical process of DOCu uptake and carbon fixation efficiency in primary productivity, intelligent colorimetric detection of algal DOCu bioavailability-based speciation is proposed in this study, which is dexterously imitated by TiO_2-based photodegradation of 7 typical natural ligands (including L-methionine, urea, oxalic acid, citric acid, EDTA, D-glucuronic acid, L-glycine), the reduction of photogenerated Cu(II) into Cu(I) with HAC, and then the absorption of hydrophilic nanofibers. The deep learning model is combined with DP-based real-time colorimetric measurement of bioavailable Cu(I) concentration, using a time-lapse camera. The HSAB theory is used to discover the mechanism of the differences in the photodegradation kinetics. Hence,

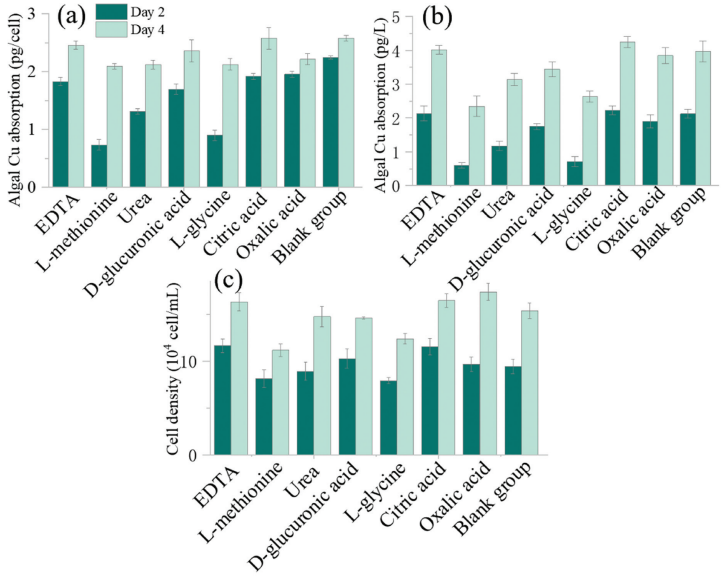

Fig. 5. Algal Cu uptake per cell on day 2, 4 (a), total algal Cu uptake on day 2, 4 (b), cell density growth with different DOCu organic ligands (c).

the biomimetic sensor-based Cu speciation assessment could predict the DOCu bioavailability and carbon fixation efficiency, *i.e.*, the Cu toxicity to aquatic organisms, Cu organic complexes that are difficult to degrade will also be difficult to absorb and even carbon fixation inefficiency.

Declaration of competing interest

The authors declare that they have no known competing financial interests or personal relationships that could have appeared to influence the work reported in this paper.

CRediT authorship contribution statement

Zhaojing Huang: Writing – original draft, Investigation, Formal analysis, Conceptualization. **Hao Li:** Writing – original draft, Software, Formal analysis. **Jiayi Luo:** Writing – original draft, Methodology, Formal analysis. **Shunxing Li:** Writing – review & editing, Supervision, Funding acquisition, Conceptualization. **Ming Zhao:** Software, Methodology. **Fengjiao Liu:** Writing – review & editing, Supervision. **Haijiao Xie:** Software.

Acknowledgments

This work was supported by the National Natural Science Foundation of China (No. 22074058, S. Li). We acknowledge the Fujian Province Key Laboratory of Modern Analytical Science and Separation Technology and Minnan Normal University for assistance with experimental and computing resource support. We also thank all members of our laboratory for valuable comments and discussions.

Supplementary materials

Supplementary material associated with this article can be found, in the online version, at doi:10.1016/j.cclet.2024.110209.

References

[1] A.P. Hollister, H. Whitby, M. Seidel, et al., Mar. Chem. 234 (2021) 104005.
[2] X. Cao, Z.X. Yu, M. Xie, et al., Environ. Sci. Technol. 57 (2023) 1060–1070.
[3] F. Liu, C. Fortin, G.C. Peter, et al., Environ. Sci. Technol. 52 (2018) 7988–7995.
[4] L. Kong, N.M. Price, Limnol. Oceanogr. 65 (2020) 601–611.
[5] L. Kong, N. Price, Environ. Sci. Technol. 56 (2022) 9103–9111.
[6] D. Lu, Q. Liu, M. Yu, et al., Environ. Sci. Technol. 52 (2018) 1088–1095.
[7] J. Sýkora, Coord. Chem. Rev. 159 (1997) 95–108.
[8] P. Sánchez-Marín, E. Aierbe, J.I. Lorenzo, et al., Aquat. Toxicol. 178 (2016) 165–170.
[9] K.N. Buck, J. Moffett, K.A. Barbeau, R.M. Bundy, et al., Limnol. Oceanogr. 10 (2012) 496–515.
[10] H. Whitby, C.M.G. van den Berg, Mar. Chem. 173 (2015) 282–290.
[11] D. Sun, T. Fan, F. Liu, et al., Biosens. Bioelectron. 212 (2022) 114390.
[12] X. Liu, H. Lv, H. Xu, Chin. Chem. Lett. 26 (2015) 205–209.
[13] M.H. Lee, C.L. Osburn, K.H. Shin, et al., Water Res. 147 (2018) 164–176.
[14] M. Zoumpoulaki, G. Schanne, N. Delsuc, et al., Angew. Chem. Int. Ed. 61 (2022) e202203066.
[15] A.L. Le Sueur, R.N. Schaugaard, M.H. Baik, et al., J. Am. Chem. Soc. 138 (2016) 7187–7193.
[16] V.L. Sushkevich, O.V. Safonova, D. Palagin, et al., Chem. Sci. 11 (2020) 5299–5312.
[17] A.M. Craven, G.R. Aiken, J.N. Ryan, Environ. Sci. Technol. 46 (2012) 9948–9955.
[18] K. Ndungu, Environ. Sci. Technol. 46 (2012) 7644–7652.
[19] K. Zhu, M.J. Hopwood, J.E. Groenenberg, et al., Environ. Sci. Technol. 55 (2021) 9372–9383.
[20] Y. Zhao, X. Chang, A.S. Malkani, et al., J. Am. Chem. Soc. 142 (2020) 9735–9743.
[21] L. Aubert, N. Nandagopal, Z. Steinhart, et al., Nat. Commun. 11 (2020) 3701.
[22] S. Shi, Y. Si, Y. Han, et al., Adv. Mater. 34 (2022) 2107938.
[23] B. Chen, L. Peng, M. He, et al., Chin. Chem. Lett. 34 (2023) 107262.
[24] D. Cao, Y. Yin, Chinese Chem. Lett. 30 (2019) 650–652.
[25] Z.J. Huang, J. Luo, F.Y. Zheng, et al., Food Chem. 373 (2022) 131593.
[26] Y. Zhou, Y. Wang, W. Peijnenburg, et al., Environ. Sci. Technol. 57 (2023) 17786–17795.
[27] Y. Li, T. Hong, Y. Gu, et al., Environ. Sci. Technol. 57 (2023) 1225–1236.
[28] H. Hu, J.P. Bindu, J. Laskin, Chem. Sci. 13 (2022) 90–98.
[29] L. Guo, T. Wang, Z. Wu, et al., Adv. Mater. 32 (2020) 2004805.
[30] M.G. Haberl, C. Churas, L. Tindall, et al., Nat. Met. 15 (2018) 677–680.
[31] J. Luo, Z. Huang, S. Li, et al., Anal. Chem. 94 (2022) 14801–14809.
[32] W. Xu, W. Song, Y. Kang, Anal. Chem. 93 (2021) 12758–12766.
[33] P. Tsvetkov, S. Coy, B. Petrova, et al., Science 375 (2022) 1254–1261.
[34] S. Retelletti Brogi, C. Balestra, R. Casotti, et al., Sci. Total Environ. 733 (2020) 139212.
[35] G. Dulaquais, M. Waeles, J. Breitenstein, et al., Environ. Chem. 17 (2020) 385–399.
[36] F. Liu, Q.G. Tan, D. Weiss, et al., Environ. Sci. Technol. 54 (2020) 8177–8185.
[37] Z.J. Huang, H. Li, J.Y. Luo, et al., Analy. Chem. 95 (2023) 6156–6162.
[38] Y. Du, Q. Huang, S. Li, et al., J. Hazard. Mater. 468 (2024) 133841.
[39] B. Nowack, Environ. Sci. Technol. 36 (2002) 4009–4016.